ISBN: 978-1-948012-06-5

Contents List available at VOLKSON PRESS

World Symposium on Mechanical and Control Engineering (WSMCE)

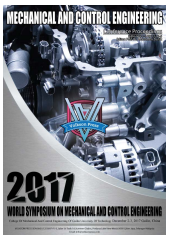

RESEARCH ON THE INFLUENCE FACTORS OF THE DROPLETS VOLUME OF JETTING DISPENSER

Qian Shen, Guiling Deng*, Can Zhou, Zhixiang Yang, Xikang Cheng

College of Mechanical and Electronical Engineering, Central South University, Yuelu Street, Changsha, China
Corresponding Author Email: gldeng@csu.edu.cn

ARTICLE DETAILS

Article History:

Received 02 october 2017
Accepted 06 october 2017
Available online 11 november 2017

Keywords

High speed dispensing, droplets volume, finite element analysis, orthogonal test

ABSTRACT

The droplets volume is an important indicator to evaluate the quality of dispensing, and there are many factors that affect the volume of droplets, such as the liquid viscosity, the fluid cavity temperature, the driving voltage of piezoelectric stacks, the rising time, the supply pressure of liquid, etc. To figure out the relationship between the influence factors and the droplets volume, this paper screened three major factors, namely the fluid cavity temperature, the driving voltage of piezoelectric stacks and the supply pressure of liquid, to study. Firstly, the temperature control system of fluid cavity was established, and the finite element analysis of the temperature field was verified, which turned out that the fluid cavity temperature stayed stable at the set value in the system. Then, the dispensing platform was built. Finally, the results of the experiment were analyzed though the range analysis method, and the results showed that the droplets volume increased with the three factors, and the fluid cavity temperature had the greatest influence on the droplets volume.

1. Introduction

Microelectronics packaging technology is the leading industry in the microelectronics, moreover, high-speed dispensing technology is the key to realize the industrialization [1-5]. Based on the advancing requirement of dispensing precision and dispensing efficiency, the dispensing technology has been changed from the traditional contact dispensing to non-contact jetting dispensing, which has a series of advantages such as no vertical displacement, wide dispensing range and high efficiency [6-11]. There are many factors affecting the droplets volume, which is strictly required in high-speed dispensing technology. However, current researches were mostly based on the control variable method to study a single influence factor. A complete test scheme will increase the number of tests, which prolongs the test period and even is difficult to achieve the expected results. Therefore, the purpose of this paper is to pick out the main influence factors, design test scheme by theory and study the impact of these factors on the droplets volume.

This paper screened three major factors for analysis, one of which is the fluid cavity temperature [12]. Droplets volume is directly related to the liquid viscosity, which increases rapidly with the rising temperature [13]. So, the temperature stability of fluid cavity must be strictly controlled in the test process. In this paper, temperature control system of fluid cavity is established and shown in Figure 1(a). Firstly, the temperature sensor detects the real-time temperature of the fluid cavity, and temperature signal is processed and sent to the control system. Then, the control system compares the temperature signal with the set temperature and outputs the control signal. Finally, the control signal is added to the heating device after being amplified, and the temperature of the fluid cavity will stay stable.

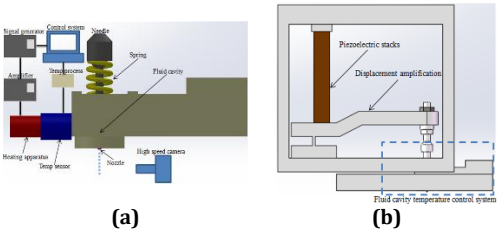

(a)

(b)

Figure 1: (a) The Temperature Control System of Fluid Cavity. (b) The Structure Model of Dispensing Valve.

The second factor to be considered is the driving voltage of piezoelectric stacks [14-17]. The structure model of dispensing valve is shown in Figure 1(b). The driving device of dispensing valve is piezoelectric stacks, which are connected with the needle through displacement amplification structure. It can be seen that the needle displacement is determined by the elongation of piezoelectric stacks, and then affects the droplets volume, while the elongation of piezoelectric stacks is linearly related to the driving voltage. Therefore, the driving voltage of piezoelectric stacks is an important factor.

The third factor to study is the supply pressure of liquid. The supply pressure of liquid directly affects the flow velocity, so the value of pressure is closely related to the droplets volume. For the above three factors, if each factor has three levels, there are 27 (3^3=27) tests in the whole test scheme, while only 9 tests in the orthogonal test scheme, which is shown in Table 1.

Table 1: Orthogonal Test Scheme

No.	Factor A	Factor B	Factor C	Test
1	1	1	1	A1B1C1
2	1	2	2	A1B2C2
3	1	3	3	A1B3C3
4	2	1	2	A2B1C2
5	2	2	3	A2B2C3
6	2	3	1	A2B3C1
7	3	1	3	A3B1C3
8	3	2	1	A3B2C1
9	3	3	2	A3B3C2

2. EXPERIMENTAL

2.1 Temperature Control System Model

The temperature control system model is composed of fluid cavity part, piezoelectric stacks part, displacement amplification part, and frame part. Among them, the fluid cavity is of an important concern, thus the grid needs to be refined. On the contrary, structures such as the small convex table and the installation hole, which have little effect on the temperature field can be simplified. Moreover, the hexahedral grid division is taken to reduce the number of nodes and the computer resources, and the grid model is shown in Figure 2(a).

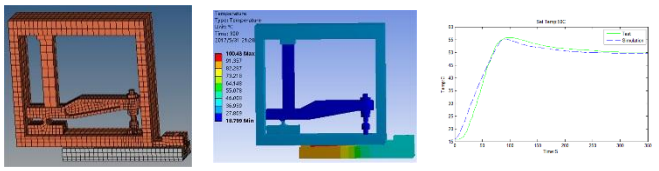

(a) (b) (c)

Figure 2: (a) Grid Model of Temperature Control System. (b) The Temperature Nephogram of Dispensing Valve. (c) Comparison between Simulation and Test Temperature of Fluid Cavity.

In order to simulate the heat transfer condition better, the contact thermal resistance is added to the contact surface. The heating device is the internal heat source of the system, and the system follows the energy conservation law,

$$-\frac{\partial q_i}{\partial x_i}+Q-\rho c\frac{\partial T}{\partial t}=0 \tag{1}$$

where q_i is a component of the heat flux vector, x_i is coordinate components, Q is heat generation power of the system, ρ is density, c is specific heat, T is temperature and t is time.

According to Fourier's Law, the heat flux is expressed as follows,

$$q_i=-\lambda\frac{\partial T}{\partial x_i} \tag{2}$$

where λ is thermal conductance.

The heat transfer follows the second boundary condition,

$$-k\frac{\partial T}{\partial \tilde{n}}=q \tag{3}$$

where $\tilde{n}$ is outward normal direction, q is thermal current intensity value.

The heat convection between system and air follows the third boundary condition,

$$\lambda\frac{\partial T}{\partial \tilde{n}}+h\left(T-T_\infty\right)=0 \tag{4}$$

where h is surface heat transfer value, T is surface temperature and T_∞ is temperature of surroundings.

Heat radiation of the system follows Stefan-Boltzmann's law,

$$\bar{q}=\delta\zeta\left(T-T_\infty\right) \tag{5}$$

where δ is Boltzmann constant, ζ is emissivity.

The temperature nephogram of dispensing valve is shown in Figure 2(b). It can be seen from the figure that the temperature is mainly concentrated in the heating device, and the temperature gradient descent at displacement from left to right. The temperature comparison of fluid cavity between the simulation and experimental test is shown in Figure 2(c). Obviously, the simulation result is in good agreement with the experimental result, which indicates that the simulation can reflect the temperature change of the fluid cavity. Furthermore, the temperature is finally stable at the set value with a tiny error.

2.2 Dispensing Platform Set Up

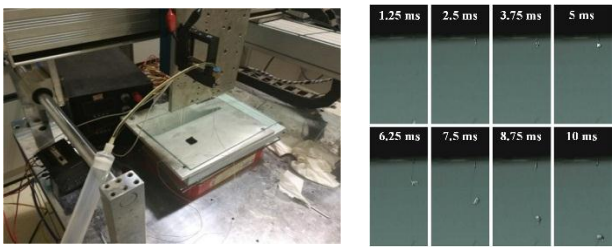

(a) (b)

Figure 3: (a) The dispensing platform. (b) A High Speed Dispensing Period. Figure 3(a) shows the dispensing platform that was built in this work. In this platform, the fluid cavity temperature is first collected by a Pt100 temperature sensor, then the temperature controller gives signal to control the on-off of load circuit, which consists of a 24V power supply, a heating device and a relay. The driving voltage of piezoelectric stacks is controlled by a signal generator and a pressure regulating valve. Meanwhile, the supply pressure of liquid is connected to an air compressor. Besides, the whole dispensing process is filmed by a high-speed camera, and a period of high speed dispensing is shown in Figure 3(b).

3 RESULTS AND DISCUSSION

3.1 Orthogonal Test Design

According to the above analysis, the basic situation of dispensing test is: frequency 100 Hz; duty ratio 50%; rising time 5 ns; cumulative time 100 s. The variable factors and levels are set in Table 2. Test results are shown in Table 3, and the first three tests were photographed by a high-speed camera as shown in Figure 4(a). According to Table 1 and Table 3, the orthogonal test table is designed and shown in Table 4.

Table 2: Variable Factors and Levels

Variable factor	Level		
	1	2	3
A: Temperature (°C)	30	40	50
B: Voltage (V)	80	100	120
C:Pressure (MPa)	0.005	0.010	0.015

Table 3: Orthogonal Test Results

No.	Temperature (°C)	Voltage (V)	Pressure (MPa)	Volume (nL)
1	30	80	0.005	20
2	30	100	0.010	39
3	30	120	0.015	42
4	40	80	0.010	24
5	40	100	0.015	65
6	40	120	0.005	46
7	50	80	0.015	72
8	50	100	0.005	44
9	50	120	0.010	76

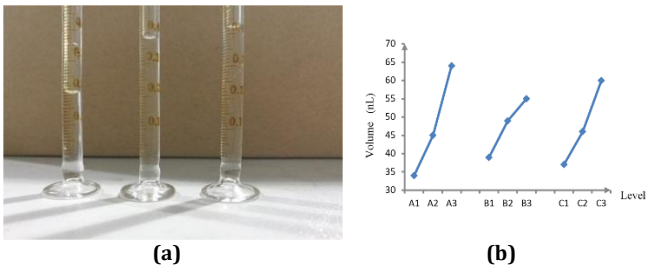

(a) (b)

Figure 4: (a) Cumulative Droplets Volume (No. 1 to 3). (b) Trend Diagram.

Table 4: Orthogonal Test Table

No.	Factor				Result
	A	B	C	Null	
1	1	1	1	1	20
2	1	2	2	2	39
3	1	3	3	3	42
4	2	1	2	3	24
5	2	2	3	1	65
6	2	3	1	2	46

7	3	1	3	2	72
8	3	2	1	3	44
9	3	3	2	1	76

3.2 Range Analysis Method

According to Table 4, the ranges of factor A, B, C are calculated and filled in as shown in Table 5, and A3C3B3 is selected as the excellent test because of the max cumulative droplets volume. The trend diagram of the factor A, B, C and the droplets volume is shown in Figure 4(b). Firstly, it can be seen that the droplets volume increases gradually with the three factors, and the growth rate of droplets volume increases with both the fluid cavity temperature and the supply pressure of liquid, while the growth rate decreases with the driving voltage of piezoelectric stacks. Secondly, the fluid cavity temperature has the greatest effect on the droplets volume, while the driving voltage of piezoelectric stacks has the least effect. Finally, as A3C3B3 is selected as the excellent test for its max cumulative droplets volume, it is necessary to do a test of A3C3B3 to compare with A3B3C2. The test result of A3C3B3 is 81 nL, which is larger than 76 nL of A3B3C2. This confirms the above analysis.

Table 5: Calculation of Range

No.	Factor			
	A	B	C	Null
K_1	101	116	110	161
K_2	135	148	139	157
K_3	192	164	179	110
k_1	34	39	37	54
k_2	45	49	46	52
k_3	64	55	60	37
Range	91	48	69	51
Order	A C Null B			
Excellent	A3C3B3			

4 CONCLUSION

In conclusion, it is certified that the fluid cavity temperature can be well stabilized at the set level through the simulation and experiments temperature control system. Furthermore, the fluid cavity temperature has the greatest effect on the droplets volume, the moderate influence factor is the supply pressure of liquid, and driving voltage of piezoelectric stacks has the least effect. The conclusion of this paper provides a method to obtain the ideal droplets volume, which can be greatly changed by changing the fluid cavity temperature, or combined with the supply pressure of liquid.

ACKNOWLEDGMENT

This project is supported by China Postdoctoral Science Foundation (Grant No. 2016M602422) and National Natural Science Foundation of China (Grant No. 51705538).

REFERENCES

[1] Kay, R., Desmulliez, M. 2012. A Review Of Stencil Printing For Microelectronic Packaging. Soldering and Surface Mount Technology, 24 (3), 38-50.

[2] Li, J., Wang, W., Xia, Y., He, H., Zhu, W. 2015. The Soft-Landing Features Of A Micro-Magnetorheological Fluid Damper. Applied Physics Letters, 106, 85.

[3] Li, J., Wang, D., Duan, J.A., He, H., Xia, Y., Zhu, W. 2017. Structural Design And Control Of A Small-Mrf Damper Under 50 N Soft-Landing Applications. Ieee Transactions On Industrial Informatics, 11, 612-619.

[4] Li, J., Zhang, X., Zhou, C., Zheng, J., Ge, D., Zhu, W. 2016. New Applications Of An Automated System For High-Power Leds. Ieee/Asme Transactions On Mechatronics, 21 (2), 1035-1042.

[5] Zhao, Y.X., Li, H.X., Ding, H., Xiong, Y.L. 2005. Integrated Modelling Of A Time-Pressure Fluid Dispensing System For Electronics Manufacturing. International Journal Of Advanced Manufacturing Technology, 26 (3), 1-9.

[6] Shizhou, L.U. 2013. Research On Automated Micro-Liquid Dispensing Technology. Jixie Gongcheng Xuebao/Journal Of Mechanical Engineering, 49, 140.

[7] Chen, X.B., Kai, J. 2005. Modeling Of Positive-Displacement Fluid Dispensing Processes. Ieee Transactions On Electronics Packaging Manufacturing, 27 (1), 157-163.

[8] Yufeng, Y., Shizhou, L., Yaxin, L. 2013. Simulation And Experiment Research Of Non-Contact Micro-Liquid Reagent Dispensing. Advance Journal Of Food Science and Technology, 5 (1-3), 514-521.

[9] Tropmann, A., Lass, N., Paust, N., Metz, T., Ziegler, C., Zengerle, R., and Koltay, P. 2012. Pneumatic Dispensing Of Nano- To Picoliter Droplets Of Liquid Metal With The Starjet Method For Rapid Prototyping Of Metal Microstructures. Microfluidics and Nanofluidics, 12 (1), 75-84.

[10] Zhou, C., Li, J., Duan, J.A., Deng, G. 2016. Control And Jetting Characteristics Of An Innovative Jet Valve With Zoom Mechanism And Opening Electromagnetic Drive. Ieee/Asme Transactions On Mechatronics, 21 (2), 1185-1188.

[11] Zhou, C., Li, J.H., Duan, J.A., Deng, G.L. 2015. The Principle And Physical Models Of Novel Jetting Dispenser With Giant Magnetostrictive And A Magnifier. Scientific Reports, 5 (8), 18294.

[12] Zhou, C., Duan, J.A., Deng, G., Li, J. 2017. Improved Thermal Characteristics Of A Novel Magnetostrictive Jet Dispenser Using Water-Cooling Approach. Applied Thermal Engineering, 112 (7), 1-6.

[13] Kumagai, K., Fuchiwaki, O. 2012. A Development Of Dispenser For High-Viscosity Liquid And Pick And Place Of Micro Objects Using Capillary Force. Key Engineering Materials, 516 (8), 48-53.

[14] Jeon, J.C., Nguyen, Q.H., Choi, S.B. 2013. The Design And Modeling Of Jetting Dispenser Actuated By Dual Piezostack Actuator. Applied Mechanics and Materials, 433-435, 72-75.

[15] Nguyen, Q.H., Choi, M.K., Choi, S.B. 2008. A New Type Of Piezostack-Driven Jetting Dispenser For Semiconductor Electronic Packaging: Modeling And Control. Smart Materials and Structures, 17, 015-033.

[16] Jeon, J.C., Hong, S.M., Chung, J.U., Choi, S.B. 2015. Experimental Evaluation Of A Dual Piezostack-Driven Jetting Dispenser System. Applied Mechanics And Materials, 742 (2), 594-597.

[17] Lu, S., Liu, Y., Yao, Y., Sun, L., Zhong, M. 2014. Bond-Graph Model Of A Piezostack Driven Jetting Dispenser. Simulation Modelling Practice and Theory, 49 (1), 193-202.